

(THRU)

N68-25622

(CODE)

03

(CATEGORY)

(PAGES)

36

(NASA OR TX OR AD NUMBER)

TX-59794

FACILITY FORM 602

SILICON SOLAR CELLS FOR NEAR-SUN MISSIONS

J. V. Foster, A. C. Wilbur
Ames Research Center, NASA
Moffett Field, California 94035

D. C. Briggs
Philco Corporation
Western Development Laboratories
Palo Alto, California 94303

and

S. Friedlander
Solid State Laboratory
Electro-Optical Systems, Inc.
Pasadena, California 91107

GPO PRICE \$

CFSTI PRICE(S) \$

Hard copy (HC)

Microfiche (MF)

306

165

ff 653 July 65

INTRODUCTION

The Ames Research Center of NASA has management responsibility for a new series of Pioneer spacecraft. The first of five funded spacecraft, Pioneer VI, was launched on December 16, 1965 to obtain information on particles and fields and other solar phenomena in interplanetary space between earth and 0.8 AU of the sun. Several series of follow-on missions are proposed to extend the penetration toward the sun into the vicinity of 0.4 AU (6.25 suns) and then into 0.2 AU (25 suns), using the basic Pioneer spacecraft modified to account for the increased solar flux.

The present Pioneer spacecraft uses silicon n on p solar cells mounted on the outside of a spinning cylindrical structure. This solar cell arrangement was examined at Ames for the close-sun missions with the principal problem being exposed as the increase in cell temperature and attendant decrease in operating voltage and power due to the increase in solar flux. For the 0.4-AU mission, it appeared feasible to control the cell temperature by means of highly reflective coatings and/or selective filters, possibly in combination with a voltage booster. This approach could not be extended to 0.2 AU because of the practical problem of supplying essentially constant power from 1.0 AU (near-earth condition) to 0.2 AU from the sun. As a possible solution, the concept shown in figure 1 was evolved at Ames which utilizes a despun heat shield with an adjustable width slot for exposing the solar cells to the sun. Although the heat shield provides a means of temperature control and, consequently, the power output, it is desirable that, as the spacecraft approaches 0.2 AU of the sun, the solar cells produce the maximum possible power output during their brief exposure to the high solar flux as the cells pass under the slot. Unfortunately, most solar cells have been designed for conditions near 1 AU and do not exhibit the power output characteristic desired at high solar flux.

For the above reasons, two studies were conducted: one directed toward an investigation of highly reflective coatings and selective interference filters for solar cells on a spinning spacecraft for the 0.4-AU mission; the other, to the design, fabrication, and test of cells which would exhibit maximum operating voltage and power under conditions of high temperature and solar flux encountered in a 0.2-AU solar mission. The results of these two studies are given herein with emphasis given to the reporting of test measurements.

STUDY OF TEMPERATURE-CONTROL COATINGS AND FILTERS

Temperature-Control Coatings

In the first of these studies,¹ the use of selective interference filters and highly reflective coatings to improve solar cell performance at high insolation levels was investigated. The experimental configuration simulated a spinning spacecraft with solar cells bonded to, but thermally isolated from, the spacecraft. Measurements were made at 1, 3, and 6 air-mass-zero suns.

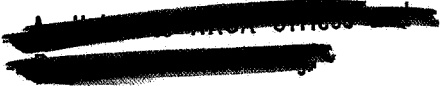
Coating Characteristics

Two types of coatings were investigated: multilayer interference coatings and opaque, fractional-area, high-reflectivity coatings.

Interference Filters: Interference filters, by selectively passing a portion of the solar spectrum, reduce the total energy incident on solar cells. As usually applied, filters reject portions of the spectrum that are not converted or that are converted with poor efficiency by the solar cell. Since the total energy absorbed is reduced without change to emissivity, the operating temperature will decrease. This improves the efficiency of conversion of wavelengths passed by the filter. The objective is to use a filter bandpass which allows more gain in cell conversion from temperature decrease than it loses from the rejected wavelengths.

Six different bandpasses were investigated for usefulness in 0.4-AU missions. Table I shows measured characteristics of each filter type at normal and off normal incidence. Filter types 1, 2, and 3 have a bandpass narrower than the total solar cell response bandwidth. Filter 4 is essentially a "blue" filter while filter types 5 and 6 closely approximate the silicon solar cell response bandwidth.

¹The study was performed by Philco Corp., WDL Division, Palo Alto, California, for the National Aeronautics and Space Administration, Ames Research Center, Moffett Field, California, under Contract NAS7-409, Donald C. Briggs, Chief Investigator.



Reflective Coatings: An opaque reflective coating applied to the underside of the cover glass and covering a fractional area of the solar cell also reduces the total energy reaching the cell without changing emissivity. Cell temperature is thereby reduced and wavelengths convertible by the cell are more efficiently converted. An advantage is realized if the improved conversion efficiency offsets the loss of conversion in the covered fraction.

Metallic silver coatings covering 20% and 40% of solar cell area were investigated. The measured reflectivity was approximately 0.8.

If these coatings can be used in place of filters for actual missions, there is significant cost advantage.

Experimental

Solar cells with cover plates were mounted on rotatable fixtures as shown in figure 2. This arrangement simulated the anticipated thermal coupling between solar cell and spacecraft. The rotating solar cell tests were performed in a vacuum chamber at a pressure of approximately 5×10^{-6} torr and at a spin rate of 43 rpm. Figure 3 shows the rotating assembly mounted in the vacuum chamber. It also shows the carbon-arc solar simulator source and the liquid nitrogen cooled shroud which thermally simulates space. During operation, the cell assembly rotation was reversed every 120 turns so that the electrical leads could wrap and unwrap, thus eliminating the need for slip rings.

Solar cell performance at thermal equilibrium with each of the six filter types was measured while rotating in the above experimental setup. In addition, tests were conducted using reflective coating area fractions of 20 and 40% coverage. The coatings were applied completely covering the long dimension perpendicular to the cell grid lines.

Results

Table II summarizes the test results at the three designated flux levels for the six different interference filters and for two different reflective coating fractions. T_{smk} shows the cold wall temperature; T_{cell} is the cell equilibrating temperature; I_{sc} is the short circuit current at the peak of the cycle, that is, when the cells were normal to the solar beam. E_{oc} is the open circuit voltage and P_{peak} the peak power under the same conditions. Figures 4, 5, and 6 show plots of the current-voltage curves for selected test specimens. In figure 7, solar cell current values from rotation under 1 sun illumination are shown for several load resistances.

Discussion

From table II it is apparent that no one of the filters or reflective coating fractions is ideal for the mission contemplated. The narrow band filters (nos. 1, 2, and 3) and the high cutoff filter (no. 4) provide good thermal control and favorable power output at 6 suns. This is at the penalty of low power at 1 sun. The wide band filters (nos. 5 and 6) show much higher temperatures as well as lower output at 6 suns; however, their performance was better at 1 sun. The two reflective coatings show inferior performance at 6 suns compared to the narrow band filters but show a better balance of power from 1 sun to 6 suns.

The results of this program have been interesting and promising. Some further study appears desirable to show the degree of solar approach for which coatings can provide a complete solution to the solar cell power problem. Optimization of filter bandpass, reflective coating fraction, or a combination of the two will be required for specific missions.

SILICON CELLS FOR HIGH SOLAR FLUX

A separate study² was made of the requirements and fabrication techniques for silicon solar cells for use between 1 AU and 0.2 AU from the sun. The study was based on the state-of-the-art capability to produce n on p silicon cells having characteristics optimized for the mission.

The problem was to design and fabricate a cell that would exhibit the maximum open-circuit voltage under conditions of high temperature and high radiation density while, at the same time, not unduly reducing the maximum short-circuit current when the cell is operated at 1 AU from the sun.

Solar cell design criteria were developed and a design established in accordance with the criteria. A number of solar cells complying with the design were fabricated. Tests made according to a predetermined test plan showed that the cells so designed and fabricated were superior to standard cells currently being employed for 1-earth-radius missions in their power conversion efficiencies at 0.2 AU.

²The study was made by Electro-Optical Systems, Inc., Pasadena, California, for the National Aeronautics and Space Administration, Ames Research Center, Moffett Field, California, under Contract NAS2-3613.

Solar Cell Design Criteria and Rationale

Series Resistance of Solar Cell: Wolf and Rauschenbach (ref. 1) have shown that series resistance is a limiting factor in the output efficiency of cells at high illumination levels. An exhaustive study of the effect of series resistance has been published by Berman (ref. 2). From the equivalent circuit in figure 8, he has derived an expression for the total series resistance given by:

$$R_s = \frac{R_c}{1 + (R_c/R_p)} + R_1 + R_6 + R_7 + R_8 \quad (1)$$

where

$$R_c = \frac{\left[1 + \frac{R_1}{R_3 + (1/2)(R_2 + R_5)} + \frac{R_1}{R_1 + R_2 + R_4} \right] (R_2 + R_4)}{2 + \frac{R_1 + R_2 + R_4}{R_3 + (1/2)(R_2 + R_5)}} \quad (2)$$

$$R_p = \frac{2R_c(R_c + R_1)}{(n - 1)(2R_c + R_1)} \quad (3)$$

This circuit represents a unit cell and takes into account all the resistances in the vicinity of one grid of a gridded cell. For a cell having several grids, the number of grids is substituted for n in Eq. (3) in performing the calculation. Using Eq. (1), with calculated or estimated values for the various values of the resistances, the following considerations were made:

Dopant Identity and Concentration: The resistivity of the bulk material of the cell enters into the series resistance calculation through the R_6 term. If nominal 1 Ω -cm is considered, $R_6 \approx 0.012 \Omega$. To consider resistivities lower than 1 Ω -cm would not appreciably reduce the total series resistance below 0.1 Ω since it can be seen later that $R_s - R_6 \approx 0.08$ to 0.1 Ω . Also, since the short-circuit current I_{sc} is directly proportional to the resistivity of the starting material, the use of material having a resistivity much less than 0.5 Ω -cm would not be warranted.

The doping impurity in the material considered was boron, since no particular advantage (such as radiation resistance) would be gained by using group III elements other than boron.

Cell Thickness: Since R_6 must be minimized, the cell should be as thin as possible. However, the thinnest a cell could be, and still be capable of absorbing close to 100% of incident photons, is 200 μ . It has been shown that in this thickness silicon absorbs 100% of photons with 0.9 μ wavelength and 94% of photons with 1.0 μ wavelength (ref. 3).

Furthermore, cells thinner than 200 μ would be very susceptible to breakage during processing. Consequently, the cell thickness should be $\geq 200 \mu$.

Diffusion Process: The diffusion program employed was similar to that used in the production of standard n on p cells. The surface to be diffused was etched, and the phosphorous source was vaporized P_2O_5 in a neutral carrier gas. The diffusion temperature was 900° C.

The sheet resistance R_S of an n layer so diffused is a prime factor in the value of series resistance of the cell. In Eq. (1), it enters into terms R_4 and R_5 . The term R_S can be defined as

$$R_S = \frac{\bar{\rho}}{t}$$

where

$\bar{\rho}$ = average resistivity of the diffused layer
 t = diffusion depth

Clearly, one would want to minimize R_S by lowering $\bar{\rho}$ or diffusing deeper. However, since a surface concentration of 10^{21} phosphorous atoms per cm^3 is the maximum impurity concentration attainable at the diffusion temperature, corresponding to a $\bar{\rho}$ of $\approx 0.001 \Omega\text{-cm}$, the only other method of decreasing R_S is to increase t by diffusing deeper. Diffusion at a higher temperature is not desirable since a noticeable decrease of minority carrier diffusion length would then occur, with a consequent decrease in the conversion efficiency of the cell. By diffusing for a longer period of time, t can be increased. Diffusing too deeply could decrease the sensitivity of the cell to the blue portion of the spectrum. Berman (ref. 2) has shown that deeply diffused n on p cells are not as sensitive to loss of blue response as are p on n cells. In his experiments, n on p cells having junctions up to 0.8 μ were as efficient in energy conversion as cells with a junction depth of 0.3 μ . In performing the calculations of Eq. (1), cells with sintered contacts having an R_S of 40 Ω per square (junction depth of 0.3 μ) would have a total series resistance of 0.2 Ω . Assuming an R_S of 15 Ω per square (junction depth of 0.8 μ), the calculation yielded a series resistance of 0.12 Ω .

Grids and Contacts: Equation (1) and reference 2 indicate one could lower the series resistance to an exceedingly small value by placing many grids on the cell. However, this would reduce the active area with a consequent loss of short-circuit current and efficiency. Berman's experiments (ref. 2) show that the optimum number of grids for an n on p cell at both 100 and 316 mW/cm^2 is 11. By extrapolation, it was assumed that 11 grids would be optimum for the much higher intensities on a close-in solar mission.

Berman has also shown that the lowest series resistance attainable with nickel-plated contacts is $\approx 0.2 \Omega$ with any number of grids greater

than 13. However, sintered silver-titanium contacts consistently provide lower series resistances than plated contacts for the same number of grids and all other variables being equal. This is due to a lower semiconductor-to-metal contact resistance, which enters into Eq. (1) through terms R_2 and R_7 . Therefore, from this evidence and from the preceding section, it can be assumed that a cell with 11 grids and a contact stripe along the 2-cm side of the cell (these contacts being formed by the sintered silver-titanium process) would have a series resistance of $\approx 0.12 \Omega$ and is the optimum type of cell for use at high intensities.

To support the above discussion on cell design for low series resistance, measured values for various combinations of design parameters compared to calculated values are shown in table III.

Radiation Resistance: Numerous studies have shown that n on p cells are more radiation resistant than p on n cells made from base material of the same resistivity. Therefore, n on p cells were chosen for this work.

The relation of base resistivity to radiation resistance was not considered in cell design.

Cell Size: This study chose 1×2 cm cells over 2×2 cm cells largely because of the lack of published data on 2×2 cm cells.

Summary of Cell Requirements and Specifications: To recapitulate, the requirements for the solar cell can be stated as:

1. Minimization of series resistance R_s
2. Optimization of short-circuit current I_{sc} at 1.0 AU
3. Optimization of open-circuit voltage V_{oc} at 0.2 AU
4. Maximization of power delivery throughout the mission
5. Radiation resistance

In view of these requirements and the above considerations, a solar cell model was evolved with the following characteristics:

1. Type n on p, 1×2 cm
2. Base resistivity 0.2 to $1.2 \Omega\text{-cm}$, boron doped
3. Diffusion Phosphorous, junction depth ≈ 0.6 to 0.8μ
4. Contact geometry 11 grids with contact stripe along 2-cm side

Cover Glass: A transparent cover glass over the solar cell provides physical and radiation protection and reduces operating temperature by decreasing the effective α/ϵ ratio. Normally, covers are affixed to cells with an adhesive. The sensitivity of adhesives to ultraviolet and nuclear radiation is a disadvantage in the high fluxes encountered in close solar approach missions. Therefore, SiO_2 integral covers were specified.

Sample Cell Fabrication

Over 60 sample cells were fabricated for the test program. The cell specifications are given in table IV. Cell layout is shown in figure 9.

Cover Glass Application

During the integral quartz cover application portion of the fabrication of the 0.2-AU cells, problems were encountered in attempting to fabricate quartz films thicker than 25 μ . The problem evidenced itself in gross cracking and delamination of the quartz layers.

Since thicker covers will certainly be required, further work would be needed to show feasibility of integral covers.

Test Procedures and Results

Screening: All production cells were screened according to performance at 28° C under 100 mW/cm² tungsten light. All cells with short-circuit current, I_{sc} , and open-circuit voltage, V_{oc} , typical of the lot were retained for further tests.

Spectral Response: The spectral responses were measured. Figure 10 is typical of the spectral response curves for the cells tested. It can be seen that the spectral response of the EOS solar cell peaks at approximately 7000 Å, and a typical blue-shifted solar cell peaks at approximately 8000 Å. The reason for this peak wavelength response is not known at present; however, it is believed that this is caused by the stress induced into the cells by the application of the integral quartz cover glass.

Balloon Standard Cell Comparison: Three sample cells were taken to Table Mountain, California, and short-circuit current readings were recorded. The tests conducted at Table Mountain indicate that the sample cells responded in the same manner as the secondary calibrated balloon cell to spectral shifts at Table Mountain. The test results were used to calculate the value of short-circuit current of the sample cells, as shown in table V.

Temperature Coefficients of Performance: The temperature sensitivity of the electrical parameters of five silicon solar cells was measured under 100 mW/cm² tungsten light over a temperature range of 10° C to 80° C in 10° increments. The parameters measured were open-circuit voltage V_{oc} , maximum power voltage V_{mp} , maximum power P_{mp} , and short-circuit current I_{sc} . In all cases, the curves obtained for the electrical parameters measured were linear over the temperature range of +10° C to +80° C. The resultant temperature coefficients are listed in table VI.

The average open-circuit voltage of the five solar cells at 28° C was determined to be 570 mV.

Series Resistance: The series resistance of every production solar cell was measured by the technique described in reference 1. The results indicated a range of values of series resistance of less than 0.1Ω to a maximum value of 0.46Ω . From these results, eight solar cells were selected with series resistances less than 0.1Ω for use in the high intensity electrical performance testing.

Performance at High Intensity: The tungsten light performance test was used to obtain the electrical characteristic curves of these eight selected solar cells over an intensity ranging from 1 sun (140 mW/cm^2) to 10 suns (1400 mW/cm^2). (Equipment limitations prevented 25-sun testing.)

After the solar cell obtained an equilibrium temperature of $28^\circ \text{C} \pm 1^\circ \text{C}$, a voltage-current characteristic curve was taken and the following electrical parameters of the cell at the particular intensity were measured: open-circuit voltage, short-circuit current, maximum power current, maximum power voltage, and curve factor.

Four cells from the major solar cell vendors, in addition to the EOS 0.2-AU cell, were measured over an intensity range of 1 to 10 suns. The maximum power outputs versus intensity are shown in figure 11 and, as can be seen in every case of the regular cells, the power output decreases below the linear extrapolation of the 1-sun power output as intensity increases to 10 suns. Figure 12 presents a complete set of voltage-current characteristic curves for an EOS 0.2-AU cell and a standard silicon cell. It can be seen that the 0.2-AU cell retains its curve shape over the complete intensity range while the ordinary cell curve shape degrades considerably.

Tables VII and VIII show the curve factor for the various silicon solar cells tested as a function of intensity, and the open-circuit voltage versus intensity of all the cells tested. It can be seen from table VII that the 0.2-AU cell retains its high value of curve factor over the complete intensity range while the ordinary cells degrade as much as 20 to 50% in curve factor from 1 to 10 suns.

Table VIII relating open-circuit voltage versus intensity shows that the open-circuit voltage of the 0.2-AU cell increases continuously with intensity while that of the ordinary cells tends to decrease or stabilize at higher intensities.

The net result of the tungsten light performance test indicates that the cell specifically designed for 0.2-AU performance maintains a good curve shape and an actual increase in power over a linear extrapolation of 1-sun power output while cells designed for 1.0-AU missions degrade seriously in curve shape and power output at intensities greater than 6 suns.

Discussion

The test results show that the solar cells designed and produced for operation under high solar intensity show performance superior to commercial cells in this application. Assuming the temperature coefficients measured at 100 mW/cm² apply at higher illumination levels, these specially designed cells will deliver significantly greater power at higher operating voltage than will commercial cells on close solar approach missions.

These cells were produced in quantity by state-of-the-art techniques.

There are two apparent anomalies in the solar cell test data. First, the cell of Manufacturer No. 4, having a series resistance of $\approx 0.2 \Omega$ as measured at 1-sun intensity, still degrades in its power output at 10-sun intensity. EOS 0.2-AU cell no. 13-12, having a higher series resistance, $\approx 0.4 \Omega$ at 1-sun intensity, does not degrade much at 10-sun intensity, having a curve factor of ≈ 0.75 at 10 suns compared to a curve factor of ≈ 0.57 at 10 suns for the cell of Manufacturer No. 4.

The second anomaly exhibits itself in the behavior of the open-circuit voltage versus intensity of standard 1-AU cells. At higher intensities, the voltage does not increase logarithmically with intensity. Some factor modifies the exponential behavior at intensities greater than 4 suns.

CONCLUDING REMARKS

The problem of using silicon solar cells on near-sun missions is related largely to temperature control of the solar array and to maintenance of high power output at high solar flux input. Filters and reflective coatings placed on the solar cells show promise of controlling the temperature on missions to 0.4 AU of the sun with a minimum of spacecraft complexity. A despun heat shield concept for Pioneer shows promise of extending penetration to 0.2 AU of the sun. If the solar cells are designed and fabricated to optimize their characteristics for this mission, the cells can provide substantially improved performance over the usual 1-sun design.

REFERENCES

1. M. Wolf and H. Rauschenbach, "Series Resistance Effects on Solar Cell Measurements," Advanced Energy Conversion, vol. 3, 1963, pp. 455-499.
2. P. A. Berman, "High Efficiency Silicon Solar Cells, Final Report," Contract No. DA-36-039-SC-90777, Heliotek Corporation, Sylmar, Calif., July 1964.
3. Texas Instruments, "Development of Epitaxial Structures for Radiation Resistant Silicon Solar Cells, First Progress Report," Contract No. NAS5-3559, March 1962.

TABLE I

AVERAGED CUT-ON AND CUT-OFF POINTS FROM SPECTROPHOTOMETER MEASUREMENTS
(Wavelengths in μ)

	Incident angle, deg	Filter					
		1*	2*	3*	4*	5**	6**
Cut on, λ_1	0	0.405	0.590	0.701	0.810	0.390	0.405
	15	.403	.584	.694	.799	.389	.404
	30	.397	.572	.679	.777	.385	.401
	45	.390	.562	.660	.754	.378	.394
Cut off, λ_2	0	.583	.694	.810	---	1.09	1.09
	15	.577	.687	.800	---	1.08	1.09
	30	.564	.668	.777	---	1.06	1.07
	45	.534	.629	.737	---	1.01	1.02
IR Cut on, λ_3	0	1.21	1.23	1.28	---	1.47	1.49
	15	1.195	1.22	1.27	---	1.46	1.48
	30	1.16	1.19	1.21	---	1.41	1.44
	45	1.12	1.17	1.19	---	1.33	1.38

*Substrate thickness, 0.304 cm.

**Substrate thickness, 0.152 cm.

TABLE II

SUMMARY OF ROTATING SOLAR CELL TEST RESULTS

Filter	Number of suns	T _{sink} , °K	T _{cell} , °K	I _{sc} , A	E _{oc} , V	P _{peak} , mW
1	1	231	271	0.017	0.59	4
	3	218	291	.051	.55	12.8
	6	233	325	.076	.475	17.8
2	1	231	267	.015	.595	3.44
	3	218	282	.045	.56	13.1
	6	233	328	.069	.48	16
3	1	228	276	.015	.575	3.2
	3	228	280	.046	.560	13.6
	6	236	323	.095	.490	22.5
4	1	228	272	.021	.580	4.8
	3	228	284	.060	.550	16.2
	6	236	324	.105	.480	21.55
5	1	231	276	.056	.600	17.2
	3	230	291	.145	.565	29.25
	6	230	352	.128	.335	10.85
6	1	231	276	.056	.600	17.2
	3	230	287	.145	.565	29.25
	6	279	348	.128	.335	10.85
20% Coating	1	218	267	.058	.610	17.2
	3	231	285	.168	.540	37.8
	6	221	342	.076	.370	13.0
40% Coating	1	218	265	.047	.625	14.95
	3	231	283	.128	.580	26.3
	6	221	322	.088	.425	15.25

TABLE III
CALCULATED AND EXPERIMENTAL VALUES OF R_s FOR VARIOUS TYPES OF CELLS

Resistivity of base material, Ω -cm	Sheet resistance of diffused layer, per Ω square	Type of contact and number of grids	Calculated series resistance from the model of Berman (ref. 2), Ω	Measured series resistance (Berman), Ω
10	40	Nickel plated, 5 grids	0.82	0.8 to 1.0
1	20	Nickel plated, 11 grids	.25	.3
1	20	Sintered, 11 grids	.12	.12 (estimated)
.1	20	Sintered, 11 grids	.1	---

TABLE IV
CELL SPECIFICATIONS

<u>Size and type</u>
n on p, 1 by 2 by 2.5×10^{-2} cm
<u>Grid geometry and type</u>
11 grids, contact stripe along 2-cm side, sintered silver titanium
<u>Base resistivity</u>
0.2 to 1.2 Ω -cm
<u>Diffused junction depth</u>
0.6 to 0.8 μ
<u>Series resistance</u>
0.1 to 0.2 Ω
<u>Short-circuit current at AM = 1 (100 mW/cm²)</u>
≥ 40 mA
<u>Open-circuit voltage at AM = 1 (100 mW/cm²)</u>
> 0.55 V
<u>Cover glass</u>
Integral, 2.5×10^{-3} cm thick, SiO ₂

TABLE V

STANDARD CELL DATA

S/N No.	Ratio	I_{sc0}
11-3	0.782	47.31
10-6	.772	46.71
12-1	.746	45.13

Standard no. 169 $I_{sc0} = 60.50 \pm 0.11$ mA

$$\text{Ratio} = \frac{I_{sc}(\text{test cell})}{I_{sc}(\text{std. 169})}$$

$$I_{sc0} = (\text{ratio})(I_{sc0} \text{ std. 169})$$

TABLE VI

MEASURED TEMPERATURE COEFFICIENTS OF SOLAR CELL PARAMETERS

$\bar{T}(V_{oc}) = -2.306 \text{ mV}/^{\circ}\text{C}$
$\bar{T}(V_{mp}) = -2.21 \text{ mV}/^{\circ}\text{C}$
$\bar{T}(P_{mp}) = -0.0509 \text{ mW}/^{\circ}\text{C}$
$\bar{T}(I_{sc}) = 70.8 \text{ } \mu\text{A}/^{\circ}\text{C}$
$\bar{V}_{oc}(28^{\circ} \text{ C}) = 570 \text{ mV}$

TABLE VII

CURVE FACTOR ($P_{mp}/I_{sc}V_{oc}$) VERSUS INTENSITY

Sun	Cell number							
	13-11	13-3	4-4	4-5	10-4	12-7	12-3	11-4
1	0.757	0.782	0.779	0.783	0.766	0.687	0.778	0.763
2	.772	.785	.789	.788	.783	.722	.777	.778
4	.773	.779	.785	.781	.787	.730	.778	.781
6	.763	.768	.776	.772	.778	.715	.766	.773
8	.748	.759	.772	.765	.775	.708	.759	.767
10	.747	.748	.766	.754	.771	.683	.745	.756
R_S	<.1	<.1	<.1	<.1	<.1	<.1	<.1	.16

Sun	Cell number				Manufacturer number			
	14-10	7-4	13-8	13-12	1	2	3	4
1	0.724	0.763	0.750	0.770	0.729	0.762	0.700	0.777
2	.746	.770	.765	.777	.669	.751	.665	.763
4	.737	.761	.763	.781	.556	.696	.574	.720
6	.721	.733	.759	.772	.485	.638	.496	.669
8		.725	.753	.765	.441	.596	.439	.616
10		.717	.743	.747	.411	.550	.395	.569
R_S	.34	.22	.30	.40	.84	.30	.37	.20

TABLE VIII

OPEN CIRCUIT VOLTAGE (IN mV) VERSUS INTENSITY

Sun	Cell number							
	13-11	13-3	4-4	4-5	10-4	12-7	12-3	11-4
1	579	584	583	582	577	570	576	570
2	593	609	602	601	605	591	597	590
4	623	625	628	627	622	620	620	619
6	634	634	639	637	630	630	632	630
8	650	646	651	649	646	640	644	642
10	658	654	660	657	653	649	656	650
Sun	Cell number				Manufacturer number			
	14-10	7-4	13-8	13-12	1	2	3	4
1	570	572	580	571	564	560	571	580
2	598	607	608	599	571	576	588	596
4	614	622	620	620	575	589	590	600
6	628	626	633	632	572	589	595	600
8		635	649	647	570	605	601	600
10		635	650	650	569	608	593	591

FIGURE LEGENDS

Figure 1.- Despun heat shield concept for Pioneer.

Figure 2.- Solar cell test fixtures.

Figure 3.- Experimental test configuration.

Figure 4.- Current-voltage measurements for rotating solar cell assembly
with filter number 3.

Figure 5.- Current-voltage measurements for rotating solar cell assembly
with filter numbers 5 and 6.

Figure 6.- Current-voltage measurements for rotating solar cell assembly;
effect of coating area.

Figure 7.- Current as a function of incident angle for various loads;
solar cell with filter number 5 under 1 sun intensity.

Figure 8.- Equivalent resistance of a solar cell unit field.

Figure 9.- Dimensions of high intensity solar cell.

Figure 10.- Typical solar cell relative spectral response for constant
energy; temperature 28° C.

Figure 11.- Measured maximum power versus intensity; 1×2 cm cell;
temperature 28° C.

Figure 12.- Measured 1×2 cm cell characteristics at temperature of 28° C.

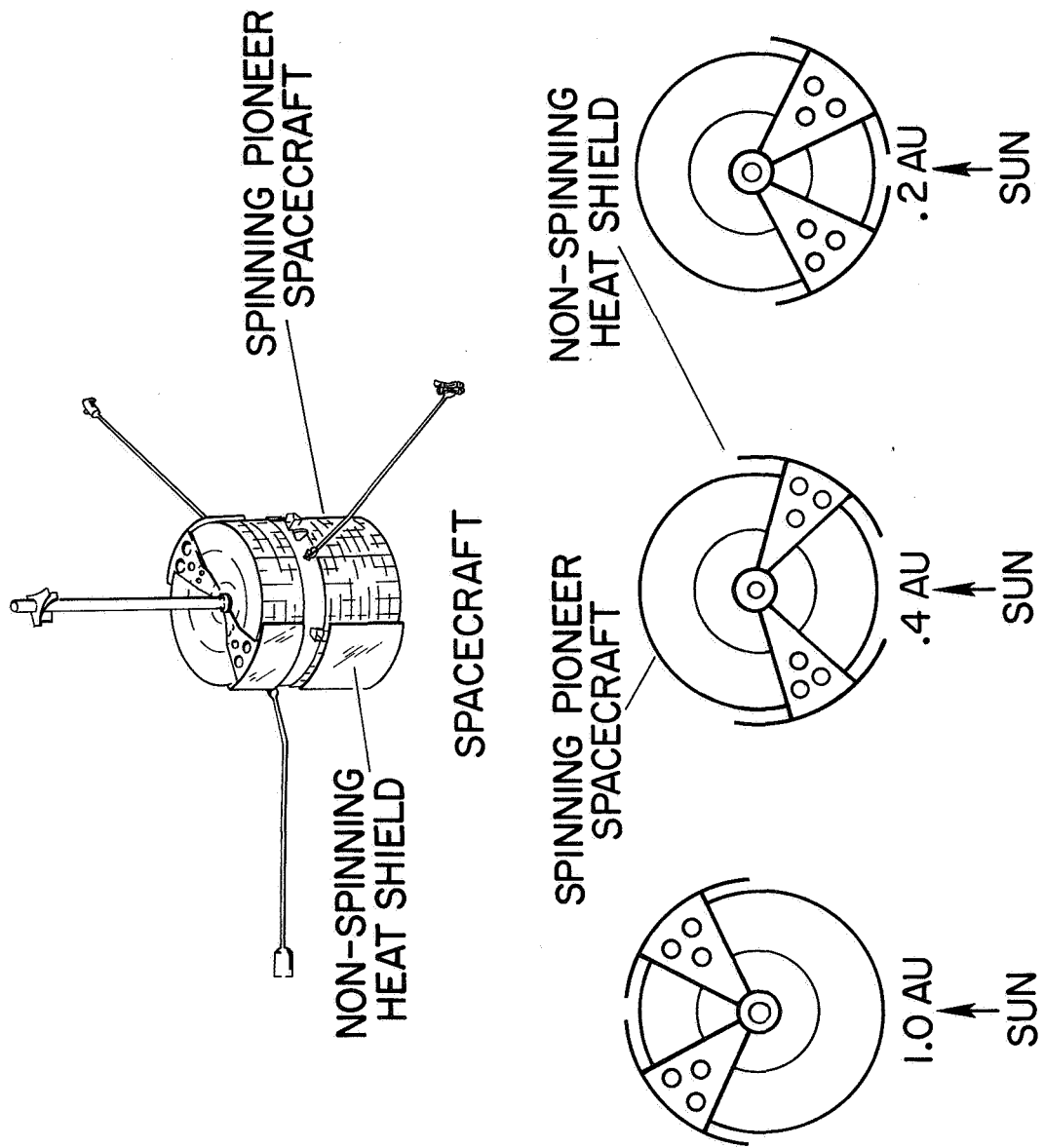


Figure 1.- Despun heat shield concept for Pioneer.

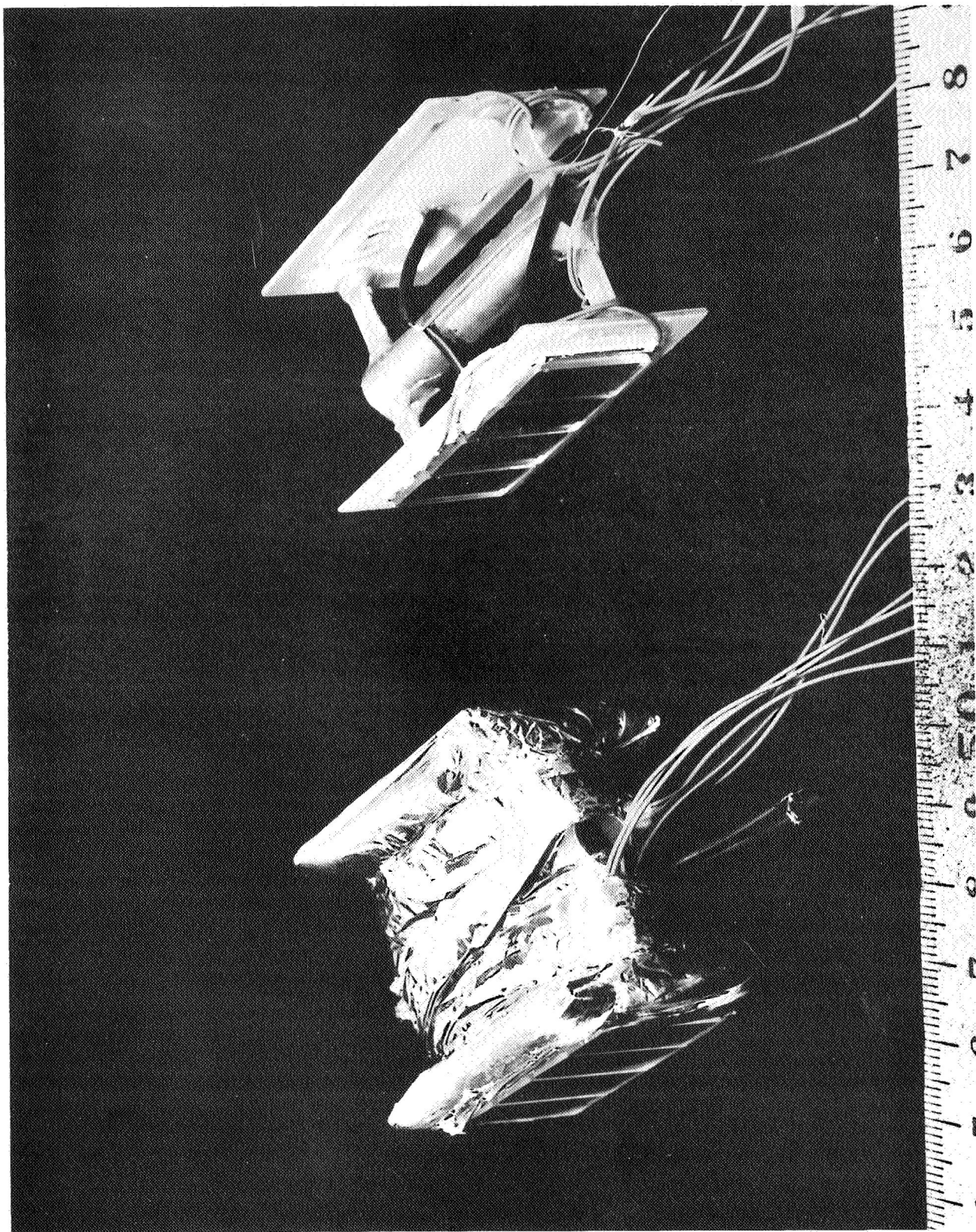


Figure 2.- Solar cell test fixtures.

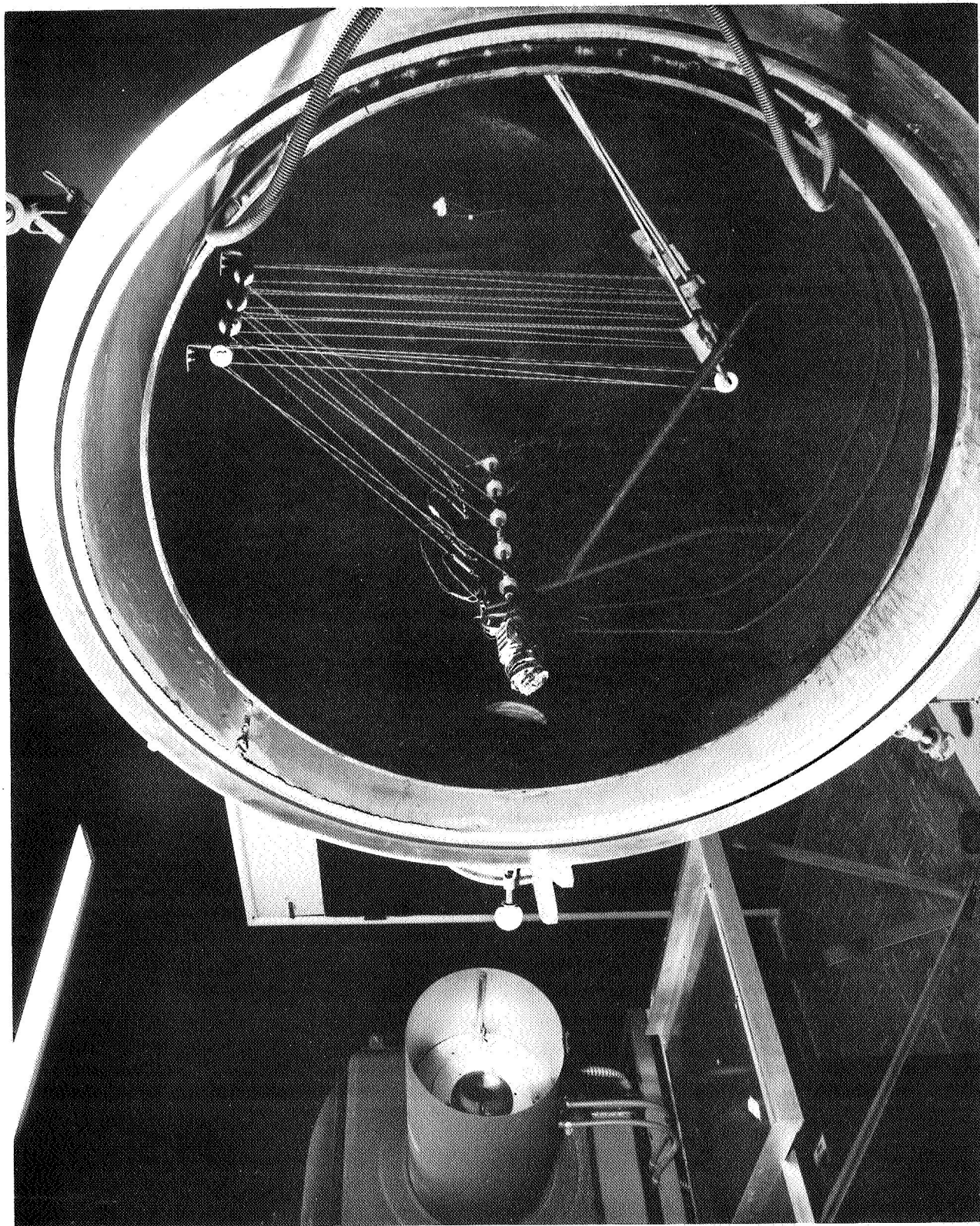


Figure 3.- Experimental test configuration.

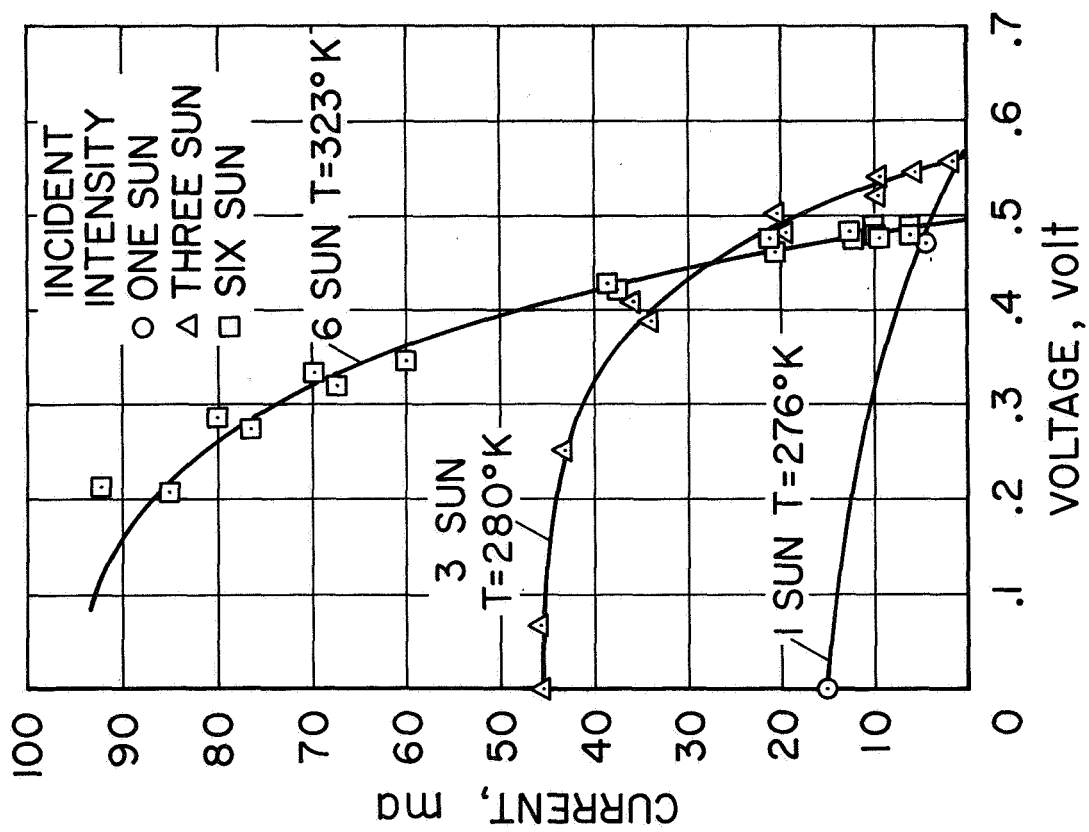


Figure 4.- Current-voltage measurements for rotating solar cell assembly with filter number 3.

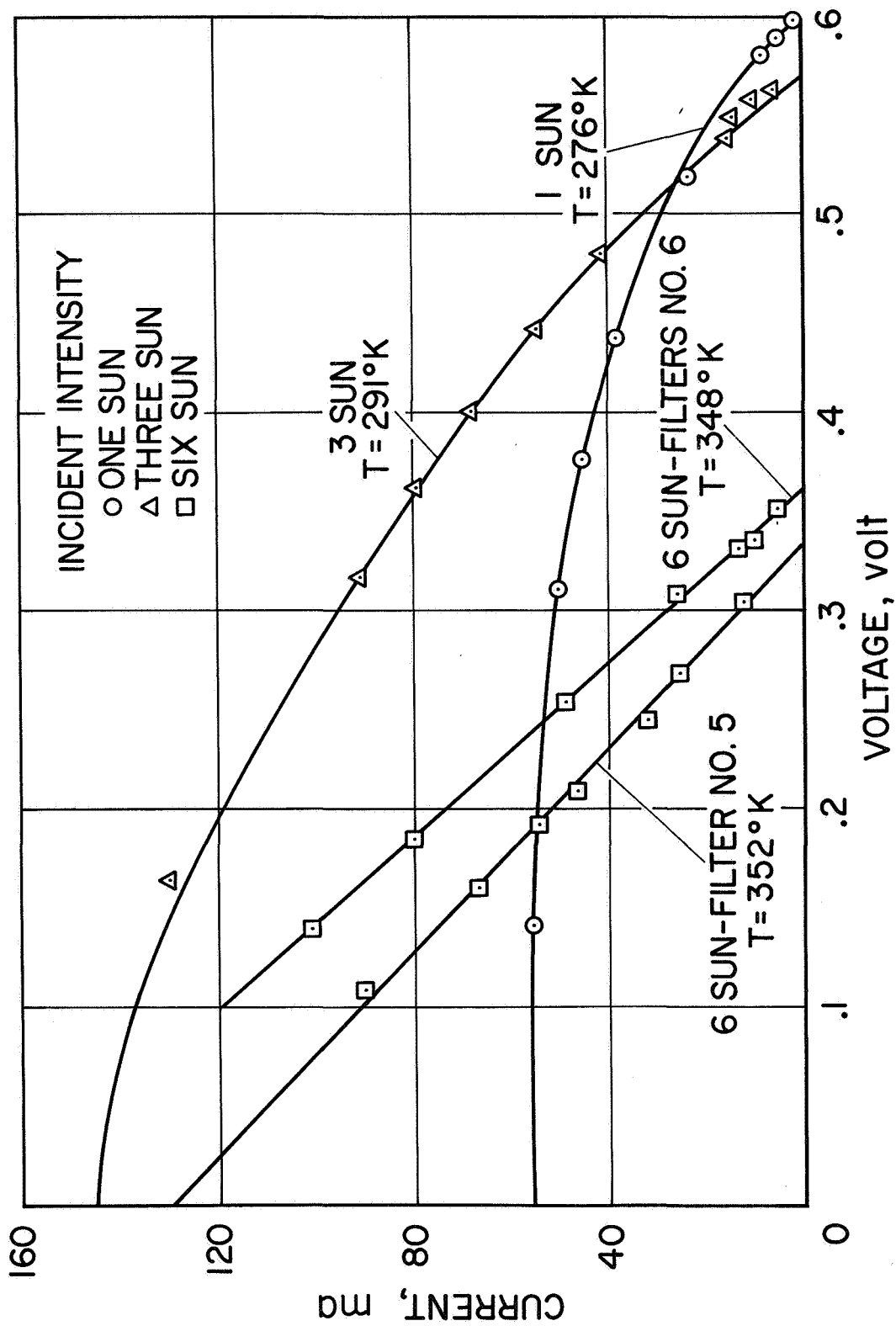


Figure 5.- Current-voltage measurements for rotating solar cell assembly with filter numbers 5 and 6.

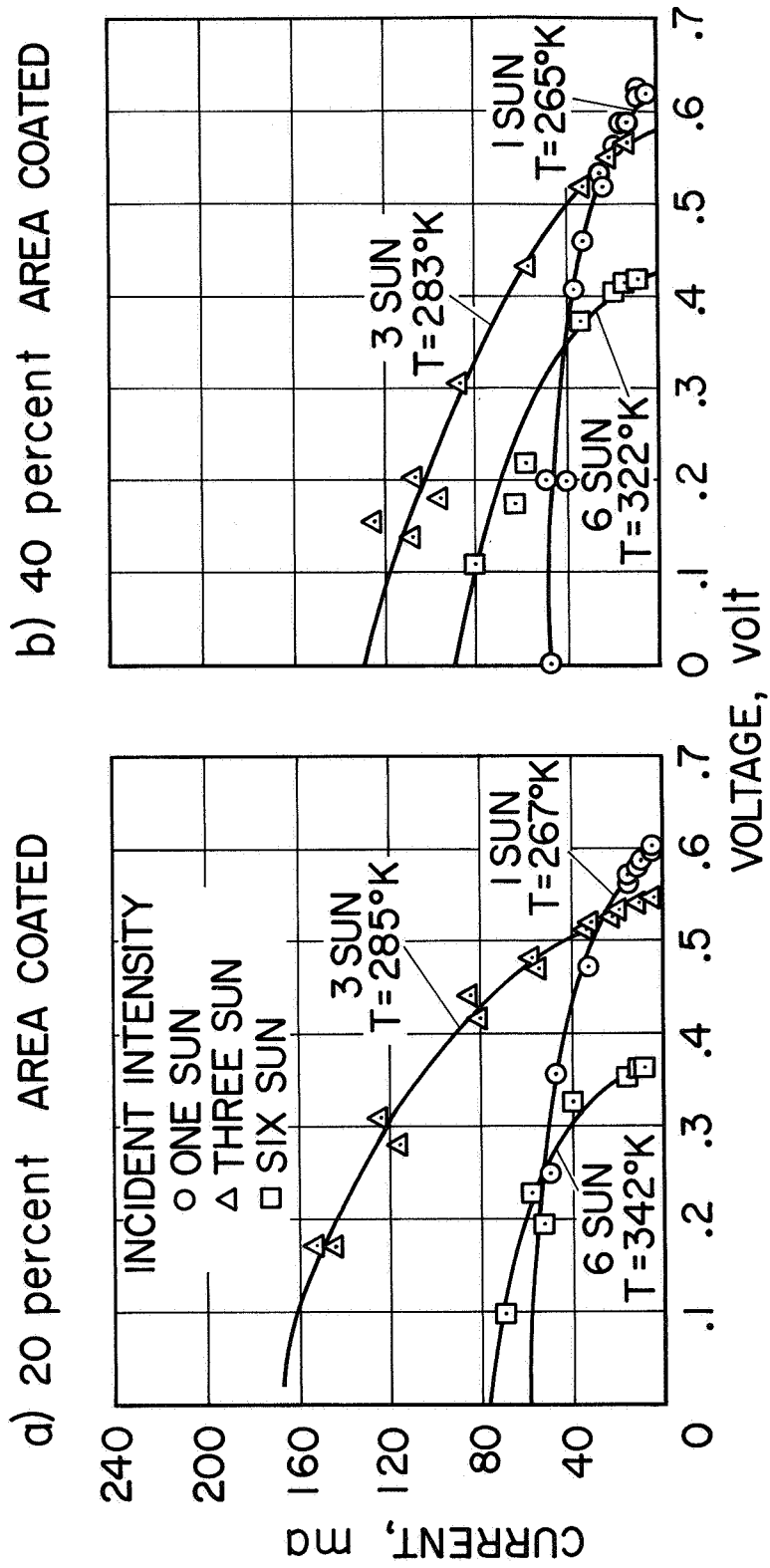


Figure 6.- Current-voltage measurements for rotating solar cell assembly; effect of coating area.

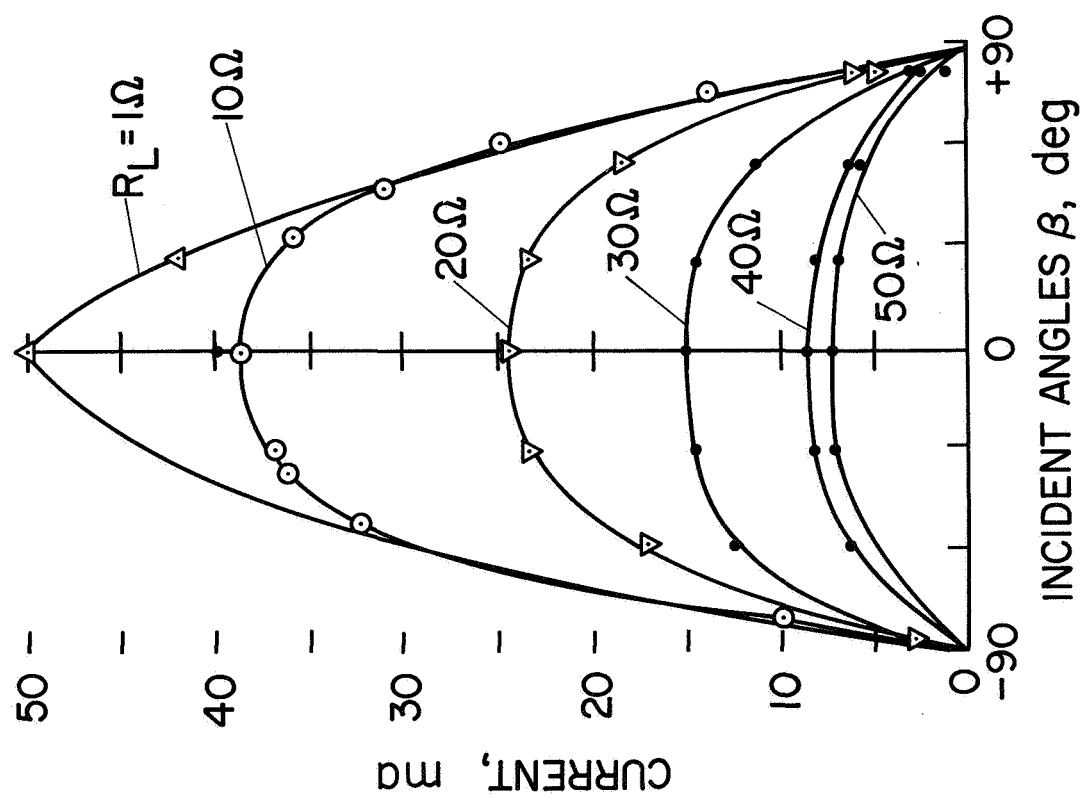


Figure 7.- Current as a function of incident angle for various loads; solar cell with filter number 5 under 1 sun intensity.

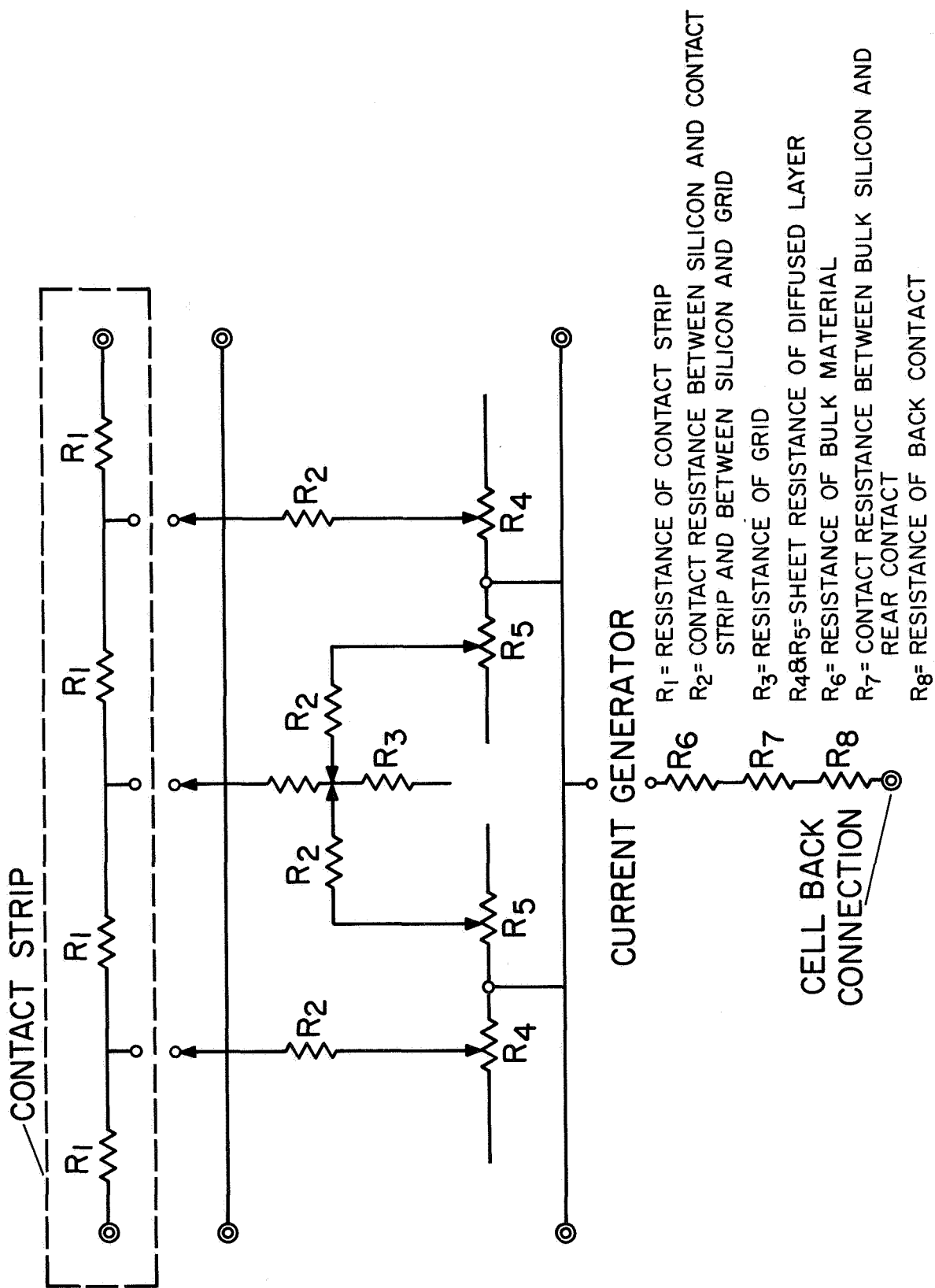


Figure 8.- Equivalent resistance of a solar cell unit field.

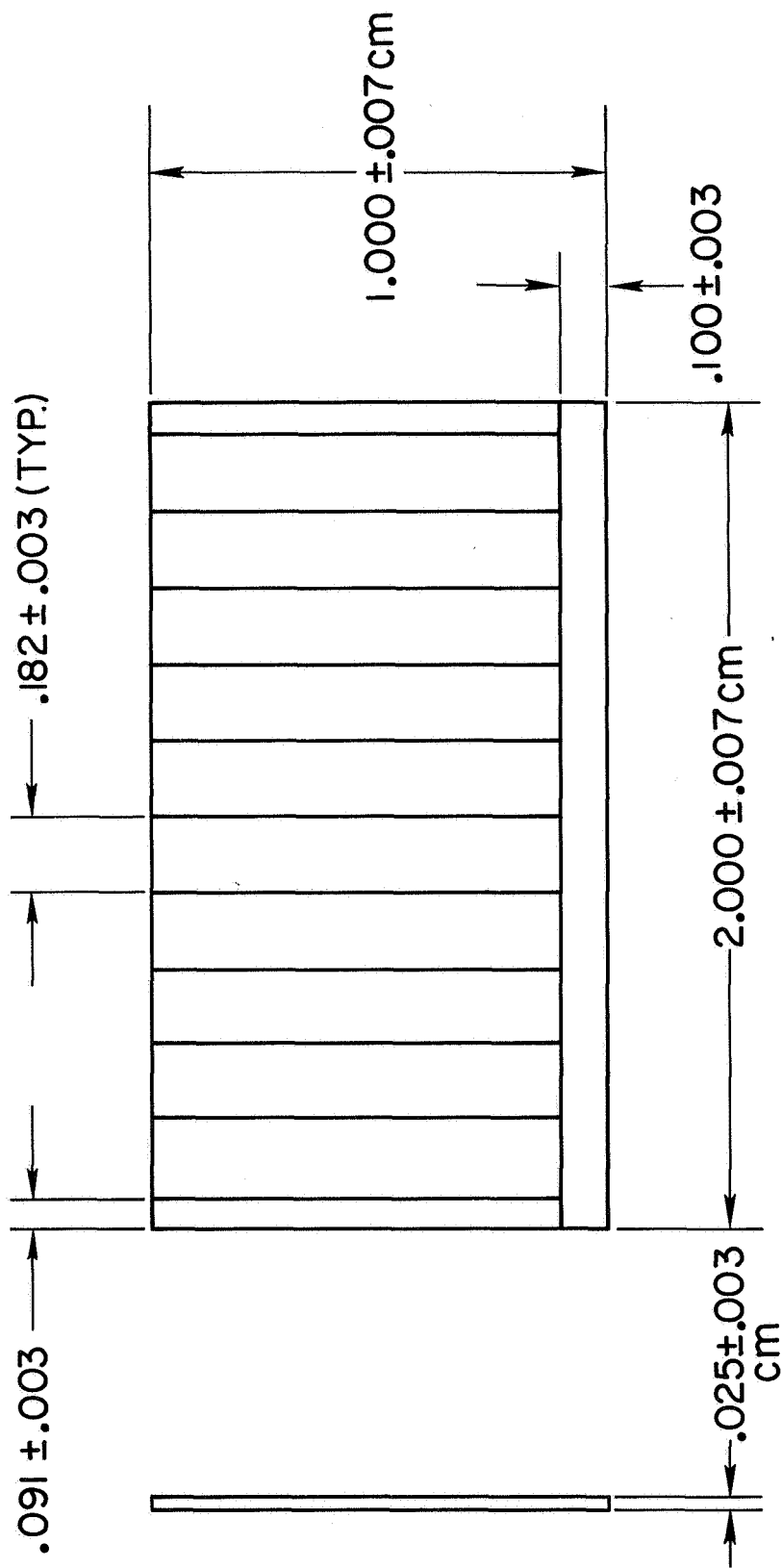


Figure 9.- Dimensions of high intensity solar cell.

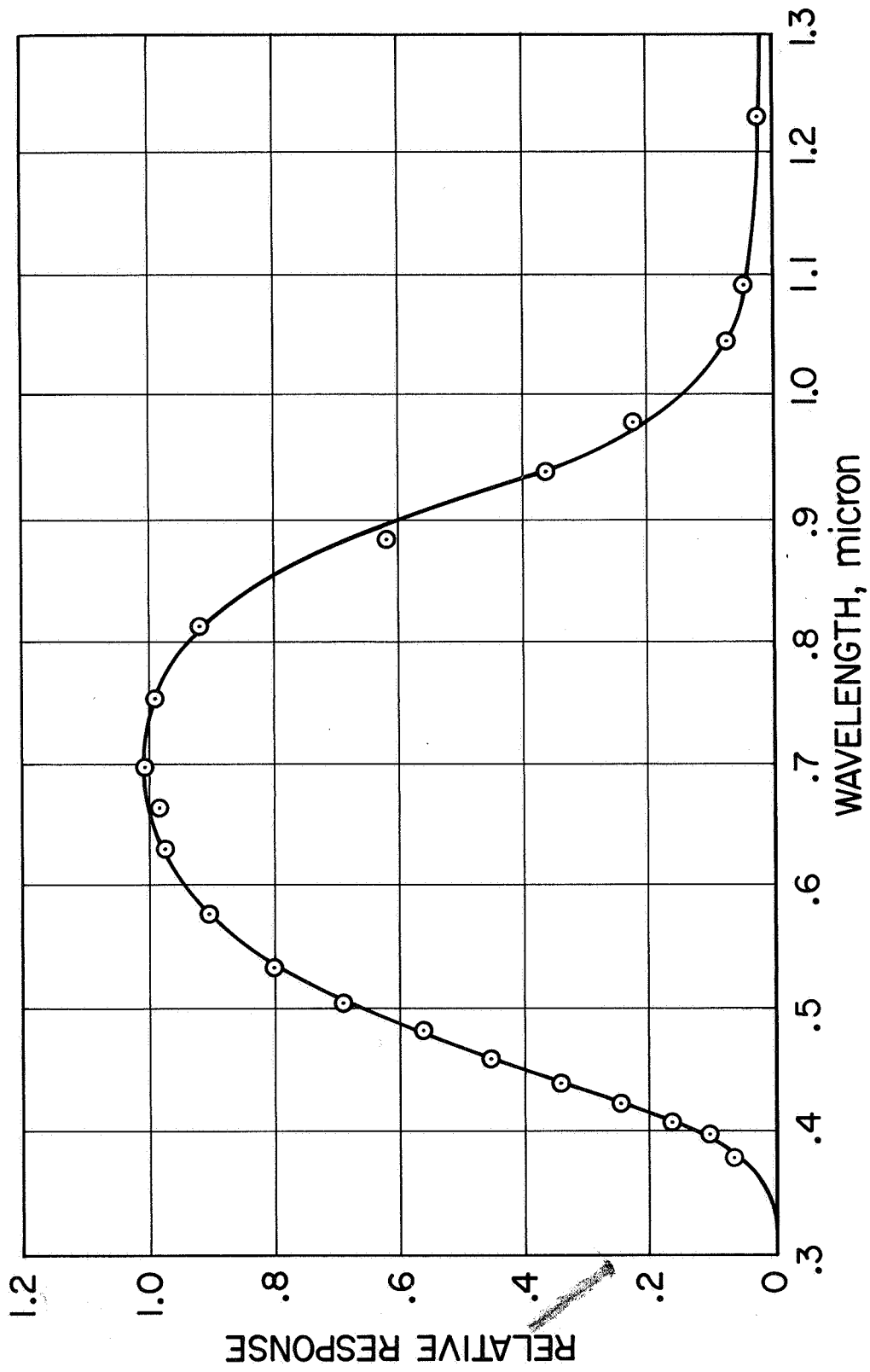


Figure 10.- Typical solar cell relative spectral response for constant energy;
temperature 28° C.

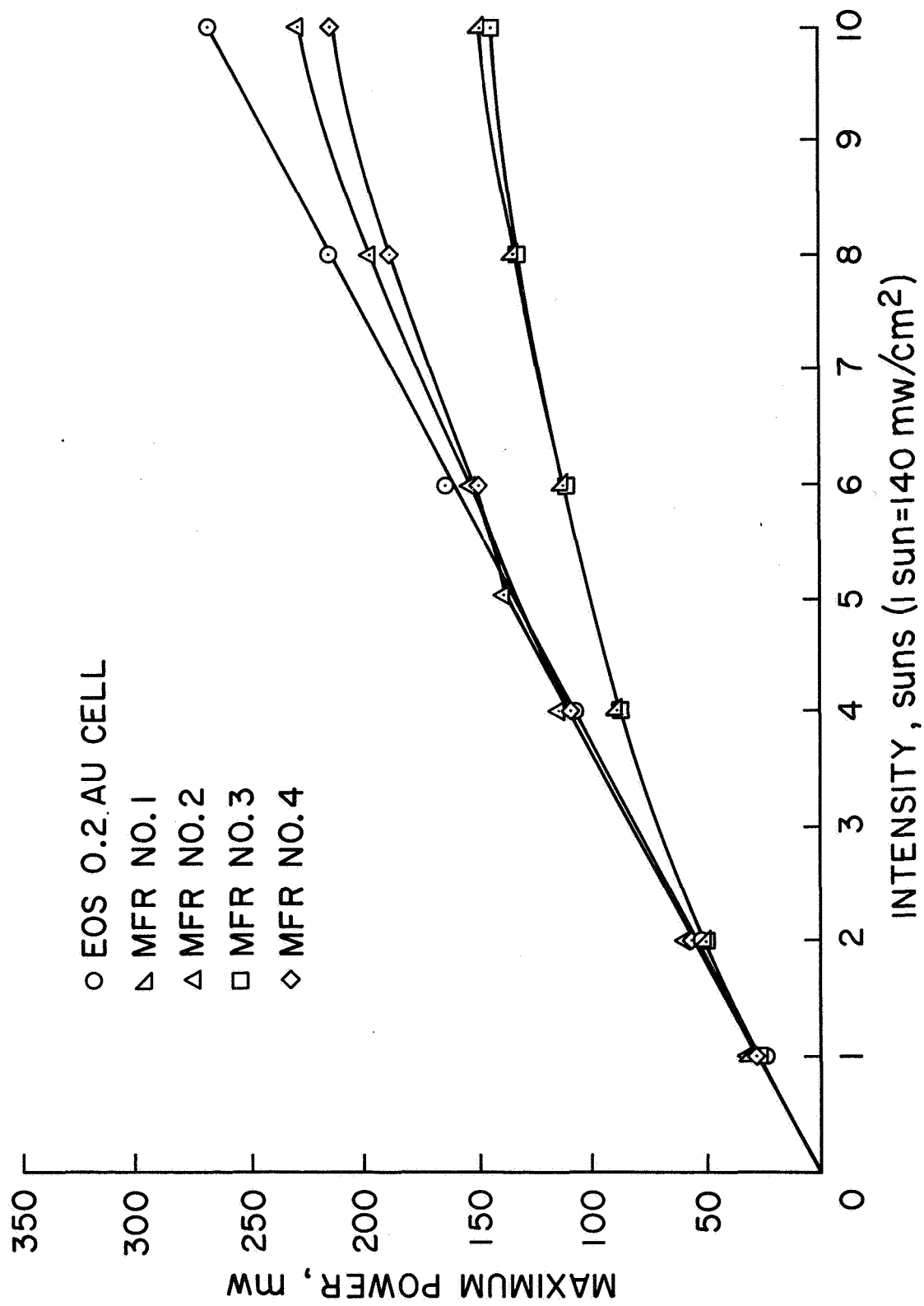


Figure 11.- Measured maximum power versus intensity; 1 x 2 cm cell.
temperature 28° C.

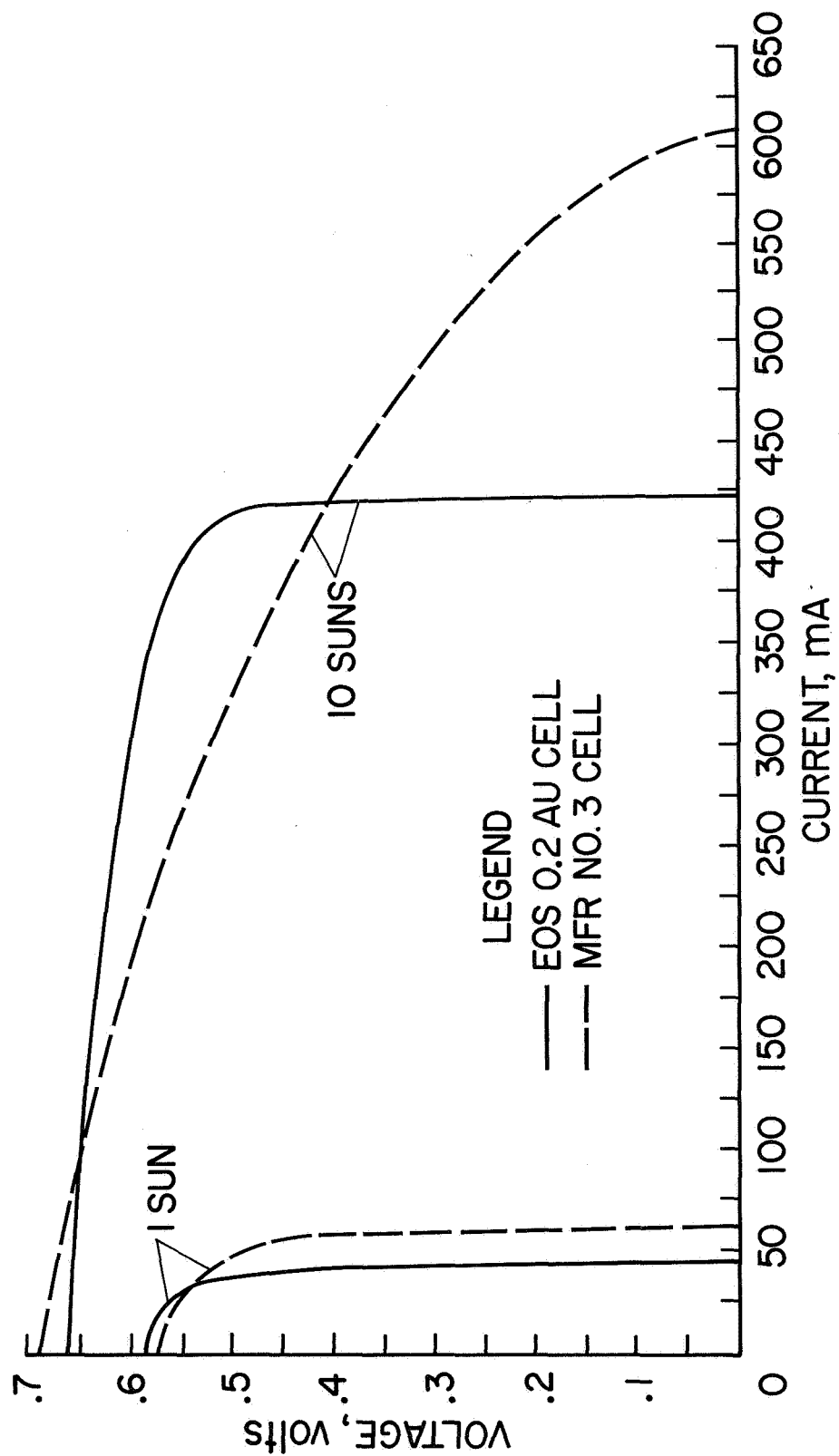


Figure 12.- Measure.. 1 x 2 cm cell characteristics at temperature of 28° C.